

Calculation of the nucleon g_1 structure function using the meson cloud model in the light-cone frame

F. Zamani and D. Saranchak*

Department of Physics, Villanova University, Villanova, Pennsylvania 19085

(Received 13 November 2000; published 9 May 2001)

We calculate polarized quark distribution functions and g_1 structure functions for the nucleon. The calculation is performed in the light-cone frame. The dressed nucleon is assumed to be a superposition of the bare nucleon plus virtual light-cone Fock states of baryon-meson pairs. For bare nucleon we consider both the case of diquark-quark clusterization and the case which there is no quark clusterization inside the nucleon. The initial distributions are evolved. The final results are compared with other theoretical calculations and experimental observations.

DOI: 10.1103/PhysRevC.63.065202

PACS number(s): 12.39.Ki, 14.20.Dh, 14.65.Bt, 24.85.+p

I. INTRODUCTION

In the late 1980's measurements by the European Muon Collaboration (EMC) indicated that only a small fraction of the proton spin is carried by the spin of the quarks [1,2]. In light of the fact that this was in disagreement with quark model prediction, a model which had great success in describing the gross features of the nucleon, the EMC result caused quite a stir in the particle physics community. This resulted in what came to be known as the "proton spin crisis" and resulted in a considerable amount of both theoretical and experimental investigation of the nucleon spin. Since then literally hundreds of papers have been published on this subject. On the experimental side, the original experiment by EMC at CERN was followed by the Spin Muon Collaboration (SMC) [3–12], also, at the Stanford Linear Accelerator Center (SLAC) [13–20] and the HERMES Collaboration at Deutsches Elektronen-Synchrotron (DESY) [21–24]. Among other things, these experiments have confirmed the original EMC result, the Bjorken sum rule (BSR) [25,26], but show the violation of Ellis-Jaffe sum rule (EJSR) [27], and what appears to be a rather large negative strange quark polarization.

On the theory side the investigation of the nucleon spin has been very active since the EMC result. The objective is to find the contribution of different sources, i.e., quarks, gluons, and orbital motion of the partons, to the spin of the proton. In the late 1980's, Altarelli and Ross [28] and Carlitz, Collins, and Mueller [29] suggested that there is a hard gluonic contribution to the first moment of g_1 structure function of the proton. Others followed up on this suggestion [30–32]. The objective here was to see whether there is a positive gluon polarization, since this would explain away the rather large negative sea polarization and rather small contribution of the quarks to the spin of the proton. For a period of time there was some apparent conflict between chiral invariant approach and gauge invariant approach to the calculation of the contribution of the gluon to the quark po-

larization. The reason being that in operator product expansion (OPE) approach, which is model independent, the hard gluons at twist-2 level make no contribution to the first moment of g_1 structure function. This apparent problem has been clarified [31,33] and now the general understanding is that there is a rather significant contribution due to gluon anomaly, which is not unexpected in PQCD regime [34]. Therefore, the observed experimental results are superposition of the quark and gluon polarizations and therefore, there is no spin crisis. For interested readers a number of excellent extended articles on this topic are in Refs. [32–44].

In Sec. II we briefly present a light-front representation of three-body systems and introduce the two types of wave functions that we will use for core nucleon. This will be followed by the formalism for the meson cloud model in Sec. III. Results and discussion will be presented in Sec. IV.

II. LIGHT FRONT REPRESENTATION OF THE NUCLEON

Since the original work by Dirac [45] several decades ago, there has been extensive use of light front frame to study high-energy processes. References [46–49] present more in depth study of the subject for the interested reader. Basic definitions and a formalism are presented in Refs. [50,51]. A four vector in light front frame is defined as

$$a = (a^+, a_-, a_\perp), \quad (1)$$

where $a^\pm = (a^0 \pm a^3)/\sqrt{2}$ and $a_\perp = (a^1, a^2)$. Following the relativistic treatment of the nucleon by Terent'ev [52,53], we separate the center of mass motion of the three quarks in nucleon from their relative motion by transforming their momenta p_1, p_2, p_3 into total and relative momenta as follows:

$$\vec{P} = \vec{p}_1 + \vec{p}_2 + \vec{p}_3, \quad (2a)$$

$$\xi = \frac{p_1^+}{p_1^+ + p_2^+}, \quad \eta = \frac{p_1^+ + p_2^+}{P^+}, \quad (2b)$$

$$q_\perp = (1 - \xi)p_{1\perp} - \xi p_{2\perp},$$

$$Q_\perp = (1 - \eta)(p_{1\perp} + p_{2\perp}) - \eta p_{3\perp}. \quad (2c)$$

*Present address: University of Maryland, College Park, MD 20742.

Then, the Hamiltonian of the system takes the form

$$H = \frac{P_{\perp}^2 + \hat{M}^2}{2P^+}, \quad (3)$$

where \hat{M} is the mass operator with the interaction term W :

$$\hat{M} = M + W, \quad (4a)$$

$$M^2 = \frac{Q_{\perp}^2}{\eta(1-\eta)} + \frac{M_3^2}{\eta} + \frac{m_3^2}{1-\eta}, \quad (4b)$$

$$M_3^2 = \frac{q_{\perp}^2}{\xi(1-\xi)} + \frac{m_1^2}{\xi} + \frac{m_3^2}{1-\xi}, \quad (4c)$$

with m_1 , m_2 , and m_3 as the constituent quarks masses. M and M_3 can be rewritten in a more transparent way in terms of the relative momenta q and Q :

$$E_1 = \sqrt{\mathbf{q}^2 + m_1^2}, \quad E_2 = \sqrt{\mathbf{q}^2 + m_2^2}, \quad E_3 = \sqrt{\mathbf{Q}^2 + m_3^2},$$

$$E_{12} = \sqrt{\mathbf{Q}^2 + M_3^2}, \quad (5a)$$

$$\xi = \frac{E_1 + q_3}{E_1 + E_2}, \quad \eta = \frac{E_{12} + Q_3}{E_{12} + E_3}, \quad (5b)$$

$$M = E_{12} + E_3, \quad M_3 = E_1 + E_2, \quad (5c)$$

where $\mathbf{q} = (q_1, q_2, q_3)$ and $\mathbf{Q} = (Q_1, Q_2, Q_3)$.

The wave function of the nucleon can be written as

$$\Psi = \Phi \chi \phi, \quad (6)$$

where Φ , χ , and ϕ are the flavor, spin, and momentum distributions, respectively. We are going to consider two different wave functions for the core nucleon. First, we assume that the nucleon is a quark-diquark system. In general, the nucleon state can be a linear combination of the following spin-isospin diquark states: (0,0), (0,1), (1,0), and (1,1). However, work done by Close [54] and Glashow [55] suggest that the spin zero diquark state will be the dominant one and therefore in the following we will only consider linear combination of spin-isospin diquark states (0,0) and (0,1). Therefore, the proton wave function can be written as

$$\Psi_1 = \frac{A}{\sqrt{2}} [uud(\chi^{\rho 1} \phi_1^{\lambda 1} + \chi^{\rho 2} \phi_1^{\lambda 2}) - udu(\chi^{\rho 1} \phi_1^{\lambda 1} - \chi^{\rho 3} \phi_1^{\lambda 3})$$

$$- duu(\chi^{\rho 2} \phi_1^{\lambda 2} + \chi^{\rho 3} \phi_1^{\lambda 3})] + \frac{B}{\sqrt{6}} [uud(\chi^{\rho 1} \phi_1^{\rho 1}$$

$$+ \chi^{\rho 2} \phi_1^{\rho 2} - 2\chi^{\rho 3} \phi_1^{\rho 3}) + udu(\chi^{\rho 1} \phi_1^{\rho 1} - 2\chi^{\rho 2} \phi_1^{\rho 2}$$

$$+ \chi^{\rho 3} \phi_1^{\rho 3}) + duu(-2\chi^{\rho 1} \phi_1^{\rho 1} + \chi^{\rho 2} \phi_1^{\rho 2} + \chi^{\rho 3} \phi_1^{\rho 3})]. \quad (7a)$$

For the second case we assume that there is no clusterization of the quarks inside the nucleon [50]:

$$\Psi_2 = \frac{-1}{\sqrt{3}} (uud\chi^{\lambda 3} + udu\chi^{\lambda 2} + duu\chi^{\lambda 1}) \phi_2. \quad (7b)$$

In Eq. (7a), $|A|^2 + |B|^2 = 1$ and in our case, with $B = -0.2$. Also, in Eq. (7), u and d represent the up and down flavor. $\chi^{\rho i}$ and $\chi^{\lambda i}$ with $i = 1, 2, 3$ represent the Melosh transformed spin wave functions [56], for example,

$$\chi_{\uparrow}^{\rho 3} = \frac{1}{\sqrt{2}} (\uparrow\downarrow\uparrow - \downarrow\uparrow\uparrow), \quad (8a)$$

$$\chi_{\downarrow}^{\rho 3} = \frac{1}{\sqrt{2}} (\uparrow\downarrow\downarrow - \downarrow\uparrow\downarrow), \quad (8b)$$

$$\chi_{\uparrow}^{\lambda 3} = \frac{1}{\sqrt{6}} (\downarrow\uparrow\uparrow + \uparrow\downarrow\uparrow - 2\uparrow\uparrow\downarrow), \quad (8c)$$

$$\chi_{\downarrow}^{\lambda 3} = \frac{1}{\sqrt{6}} (2\downarrow\downarrow\uparrow - \downarrow\uparrow\downarrow - \uparrow\downarrow\downarrow). \quad (8d)$$

The spin wave function of the i th quark is

$$\uparrow = R_i \begin{pmatrix} 1 \\ 0 \end{pmatrix}, \quad \downarrow = R_i \begin{pmatrix} 0 \\ 1 \end{pmatrix}. \quad (9)$$

In Eq. (9), R_i are the Melosh matrices

$$R_1 = \frac{1}{\sqrt{a^2 + Q_{\perp}^2} \sqrt{c^2 + q_{\perp}^2}} \begin{pmatrix} ac - q_R Q_L & -aq_L - cq_L \\ cQ_R + aq_R & ac - q_L Q_R \end{pmatrix}, \quad (10a)$$

$$R_2 = \frac{1}{\sqrt{a^2 + Q_{\perp}^2} \sqrt{d^2 + q_{\perp}^2}} \begin{pmatrix} ad + q_R Q_L & -aq_L - dQ_L \\ dQ_R - aq_R & ad - q_L Q_R \end{pmatrix}, \quad (10b)$$

$$R_3 = \frac{1}{\sqrt{b^2 + Q_{\perp}^2}} \begin{pmatrix} b & Q_L \\ -Q_R & b \end{pmatrix}, \quad (10c)$$

where

$$a = M_3 + \eta M, \quad b = m_3 + (1 - \eta)M, \quad (11a)$$

$$c = m_1 + \xi M_3, \quad d = m_2 + (1 - \xi)M_3, \quad (11b)$$

$$q_R = q_1 + iq_2, \quad q_L = q_1 - iq_2, \quad (11c)$$

$$Q_R = Q_1 + iQ_2, \quad Q_L = Q_1 - iQ_2. \quad (11d)$$

The functions $\phi_1^{\rho i}$ and $\phi_1^{\lambda i}$, with $i = 1, 2, 3$, and ϕ_2 are the

momentum wave functions, which we take to be of the following form:

$$\phi_1^{\rho i} = N_{\rho i} (X_j - X_k) \phi_1^{s i} / X_T, \quad (12a)$$

$$\phi_1^{\lambda i} = N_{\lambda i} (X_j + X_k - 2X_i) \phi_1^{s i} / X_T, \quad (12b)$$

with $i \neq j \neq k$, and [50]

$$\phi_2 = \frac{N}{(M^2 + \beta^2)^{3.5}}. \quad (12c)$$

Also,

$$X_3 = \frac{Q_\perp^2}{2\eta(1-\eta)\beta_Q^2} + \frac{q_\perp^2}{2\eta\xi(1-\xi)\beta_q^2} + \frac{m_1^2}{2\eta\xi\beta_q^2} + \frac{m_2^2}{2\eta(1-\xi)\beta_q^2} + \frac{m_3^2}{2(1-\eta)\beta_Q^2}, \quad (13a)$$

$$X_2 = q_\perp^2 \frac{(1-\eta)(1-\xi)\beta_Q^2 + \xi\beta_q^2}{2\beta_Q^2\beta_q^2\eta\xi(1-\xi)(1-\eta+\xi\eta)} + Q_\perp^2 \frac{(1-\xi)(1-\eta)\beta_q^2 + \xi\beta_Q^2}{2\beta_Q^2\beta_q^2\eta(1-\eta)(1-\eta+\xi\eta)} \\ + q_\perp Q_\perp \frac{\beta_Q^2 - \beta_q^2}{\beta_Q^2\beta_q^2\eta(1-\eta+\xi\eta)} + \frac{m_1^2}{2\eta\xi\beta_q^2} + \frac{m_2^2}{2\eta(1-\xi)\beta_Q^2} + \frac{m_3^2}{2(1-\eta)\beta_q^2}, \quad (13b)$$

$$X_1 = q_\perp^2 \frac{(1-\xi)\beta_q^2 + \xi(1-\eta)\beta_Q^2}{2\beta_Q^2\beta_q^2\eta\xi(1-\xi)(1-\xi\eta)} + Q_\perp^2 \frac{(1-\xi)\beta_Q^2 + \xi(1-\eta)\beta_q^2}{2\beta_Q^2\beta_q^2\eta(1-\xi)(1-\xi\eta)} - q_\perp Q_\perp \frac{\beta_Q^2 - \beta_q^2}{\beta_Q^2\beta_q^2\eta(1-\xi\eta)} \\ + \frac{m_1^2}{2\eta\xi\beta_Q^2} + \frac{m_2^2}{2\eta(1-\xi)\beta_q^2} + \frac{m_3^2}{2(1-\eta)\beta_q^2}, \quad (13c)$$

$$X_T = X_1 + X_2 + X_3, \quad (13d)$$

and

$$\phi_1^{s i} = \frac{1}{(1 + X_T)^{n i}}. \quad (13e)$$

In the above equations β_Q , β_q , and β are confinement scale parameters and $N_{\rho i}$, $N_{\lambda i}$, and N are normalization constants.

III. MESON CLOUD MODEL IN LIGHT-CONE FRAME

The meson cloud model has been used extensively in the 1990's, mostly to investigate the flavor asymmetry of the nucleon sea. In this approach using the convolution model, one can decompose the physical nucleon in terms of the core nucleon and intermediate, virtual meson-baryon states [57–76]. Following the work done by Holtmann, Szczurek, and Speth [69] and Speth and Thomas [72], one can write

$$|N\uparrow\rangle = Z^{1/2} \left[|N\uparrow\rangle_{\text{bare}} + \sum_{BM} \sum_{\lambda\lambda'} \int dy d^2k_\perp \beta_{BM}^{\lambda\lambda'}(y, k_\perp^2) \right. \\ \left. \times |B^\lambda(y, \vec{k}_\perp); M^{\lambda'}(1-y, -\vec{k}_\perp)\rangle \right], \quad (14a)$$

with

$$\beta_{BM}^{\lambda\lambda'}(y, k_\perp^2) = \frac{1}{2\pi\sqrt{y(1-y)}} \frac{\sqrt{m_N m_B} V_{\text{IMF}}^{\lambda\lambda'}(y, k_\perp^2)}{m_N^2 - M_{BM}^2(y, k_\perp^2)}, \quad (14b)$$

where Z is the probability of the physical nucleon being in the core state. $\beta_{BM}^{\lambda\lambda'}(y, k_\perp^2)$ is the probability amplitude for the physical nucleon with helicity $+\frac{1}{2}$ is in a virtual state consisting of baryon $B^\lambda(y, \vec{k}_\perp)$, with helicity λ , longitudinal momentum y , and transverse momentum \vec{k}_\perp , and meson $M^{\lambda'}(1-y, -\vec{k})$, with helicity λ' , longitudinal momentum $1-y$, and transverse momentum $-\vec{k}$. $V_{\text{IMF}}^{\lambda\lambda'}(y, k_\perp^2)$, is the vertex function and its explicit form for different baryon-meson pairs with their corresponding helicities are listed in the Appendix. The summations in Eq. (14) include all physically possible pairs from the pseudoscalar mesons and their corresponding baryons from baryon octet and decuplet. Using $\beta_{BM}^{\lambda\lambda'}(y, k_\perp^2)$, one can define polarized splitting function in the following way:

$$n_{BM/N}^\lambda(y) = \sum_{\lambda'} \int_0^\infty dk_\perp^2 |\beta_{BM}^{\lambda\lambda'}(y, k_\perp^2)|^2, \quad (15a)$$

$$n_{MB/N}^{\lambda'}(y) = \sum_\lambda \int_0^\infty dk_\perp^2 |\beta_{BM}^{\lambda\lambda'}(1-y, k_\perp^2)|^2. \quad (15b)$$

The splitting functions must satisfy the equations

$$n_{MB}(y) = n_{BM}(1-y), \quad (15c)$$

and

$$\langle xn_{MB} \rangle + \langle xn_{BM} \rangle = \langle n_{BM} \rangle. \quad (15d)$$

In Eq. (15d), $\langle n \rangle$ and $\langle xn \rangle$ are the first and second moments of the splitting functions. Equation (15c) ensures the global charge conservation and Eq. (15d) momentum conservation.

Calculation of the physical polarized quark distributions is similar to the procedure that was followed for unpolarized case in Ref. [76], with the following modification: To calculate the polarized core quark distribution we use the following expression [77]:

$$q_{\text{core}}^\lambda(x) = \sum_j \langle N\uparrow | P_{q\lambda}^j \delta(x-x_j) | N\uparrow \rangle, \quad (16a)$$

$$= 3 \langle N\uparrow | P_{q\lambda}^3 \delta(x-x_3) | N\uparrow \rangle, \quad (16b)$$

with

$$\sum_i x_i = 1, \quad (16c)$$

where $x_1 = \xi\eta$, $x_2 = \eta(1-\xi)$, and $x_3 = 1-\eta$, and $P_{q\lambda}^j$ is a projection operator that projects out j th quark with helicity λ and Eq. (16b) is for symmetrized wave function.

These initial distributions are calculated at some initial low Q_0^2 . In order to be able to compare our results with experiments, we evolve these initial distributions using Altarelli-Parisi equations [78] to some final high Q^2 . The Altarelli-Parisi equations for polarized distributions are [33]

$$\frac{d}{dt} \Delta q_{\text{NS}}(x,t) = \frac{\alpha_s(t)}{2\pi} \Delta P_{qq}^{\text{NS}}(x) \otimes \Delta q_{\text{NS}}(x,t) \quad (17a)$$

for nonsinglet distributions and

$$\begin{aligned} \frac{d}{dt} \Delta q_S(x,t) &= \frac{\alpha_s(t)}{2\pi} [\Delta P_{qq}^S(x) \otimes \Delta q_S(x,t) \\ &+ 2n_f \Delta P_{qG}(x) \otimes \Delta G(x,t)], \end{aligned} \quad (17b)$$

$$\begin{aligned} \frac{d}{dt} \Delta G(x,t) &= \frac{\alpha_s(t)}{2\pi} [\Delta P_{Gq}^S(x) \otimes \Delta q_S(x,t) \\ &+ \Delta P_{GG}(x) \otimes \Delta G(x,t)] \end{aligned} \quad (17c)$$

for singlet distributions. In Eq. (17) α_s is the QCD running coupling constant Δq , ΔG are the polarized quark and gluon distribution functions, ΔP 's are the splitting functions, f is the number of flavors, and t is defined as

$$dt = \ln(Q^2/Q_0^2). \quad (17d)$$

Having the polarized distribution functions one can calculate polarized singlet a_0 and nonsinglet, a_3 and a_8 distributions

and g_1^p and g_1^n polarized structure functions along with their first moment in the following way:

$$a_0(x) = \Delta u(x) + \Delta d(x) + \Delta s(x), \quad (18a)$$

$$a_3(x) = \Delta u(x) - \Delta d(x), \quad (18b)$$

$$a_8(x) = \frac{\Delta u(x) + \Delta d(x) - 2\Delta s(x)}{\sqrt{3}}, \quad (18c)$$

$$g_1^p(x) = \frac{1}{2} \left(\frac{4}{9} \Delta u(x) + \frac{1}{9} \Delta d(x) + \frac{1}{9} \Delta s(x) \right), \quad (18d)$$

$$g_1^n(x) = \frac{1}{2} \left(\frac{1}{9} \Delta u(x) + \frac{4}{9} \Delta d(x) + \frac{1}{9} \Delta s(x) \right), \quad (18e)$$

where

$$\Delta q(x) = [q_\uparrow(x) - q_\downarrow(x)] + [\bar{q}_\uparrow(x) - \bar{q}_\downarrow(x)], \quad (18f)$$

also

$$\Gamma_1^p = \int_0^1 g_1^p(x) dx, \quad (19a)$$

$$\Gamma_1^n = \int_0^1 g_1^n(x) dx, \quad (19b)$$

where Eqs. (19a) and (19b) represent the first moment of $g_1^p(x)$ and $g_1^n(x)$. Using Eqs. (18) and (19) one can calculate BSR [25,26] and EJSR [27]

$$S_B = \Gamma_1^p - \Gamma_1^n, \quad (20a)$$

$$S_{EJ}^p = \frac{1}{12} \left(a_3 + \frac{5}{\sqrt{3}} a_8 \right), \quad (20b)$$

$$S_{EJ}^n = \frac{1}{12} \left(-a_3 + \frac{5}{\sqrt{3}} a_8 \right). \quad (20c)$$

Using Eqs. (18a)–(18c) one could write polarized quark distributions in terms of singlet and nonsinglet distributions:

$$\Delta u = \frac{(\sqrt{3}a_8 + 2a_0 + 3a_3)}{6}, \quad (21a)$$

$$\Delta d = \frac{(\sqrt{3}a_8 + 2a_0 - 3a_3)}{6}, \quad (21b)$$

$$\Delta s = \frac{(-\sqrt{3}a_8 + a_0)}{3}. \quad (21c)$$

IV. RESULTS AND DISCUSSION

In Table I we present the parameters, in energy units of GeV, that have been used in Eqs. (13), (12), (16), and (17) to calculate quark distribution functions and the proton and

TABLE I. Parameters used in sets 1 and 2. Here m_u , m_d , β_Q , and β_q are all in GeV, and μ_p and μ_n are in nuclear magneton units. Set 1 represents our diquark-quark model, while set 2 represents parameters used by Schlumpf [50,51].

	m_u	m_d	β_Q	β_q	n_1	n_2	n_3	μ_p	μ_n
Set 1	0.250	0.210	0.25	0.45	2.8	2.8	2.6	2.82	-1.61
Set 2	0.263	0.263	0.607	0.607	3.5	3.5	3.5	2.81	-1.66

neutron polarized structure functions. Set 1 represents diquark-quark distribution dominated by the isoscalar diquark for the core nucleon. Set 2 is the parameters used by Schlumpf [50] and represent symmetrical distribution of quarks inside the nucleon.

In Fig. 1 we present polarized xu and xd distributions for the core nucleon. One can see the relative closeness of d_\uparrow and d_\downarrow for the diquark-quark distribution which means rather small magnitude of Δd for set 1. Having these distributions the bare nucleon is dressed up into physical nucleon by introducing the meson cloud at some initial low momentum transferred. Figure 2 shows $x\Delta u$, $x\Delta d$, and $x\Delta s$ distributions for set 1 and set 2. A couple of points concerning this graph, one is that Δd is significantly larger for set 2 compared with that of set 1 and the second point is the smallness of Δs for both sets which is expected. Figure 3 shows the details of Δs distributions which is positive, in contrast with observation (for example, see Ref. [18]). However, this is not surprising, since we have not introduced any gluon polarization at this stage. At this point we would like to mention that one can correctly infer that our model does predict asymmetries between the strange and antistrange quark distribution. However, we have shown in Ref. [76] that $\int_0^1 (s(x) + \bar{s}(x)) dx = 0$ as it should be for the nucleon. Figure 4 presents the xa_3 , xa_8 , and xa_0 distributions. These initial distributions evolve using the code of Kumano and collabora-

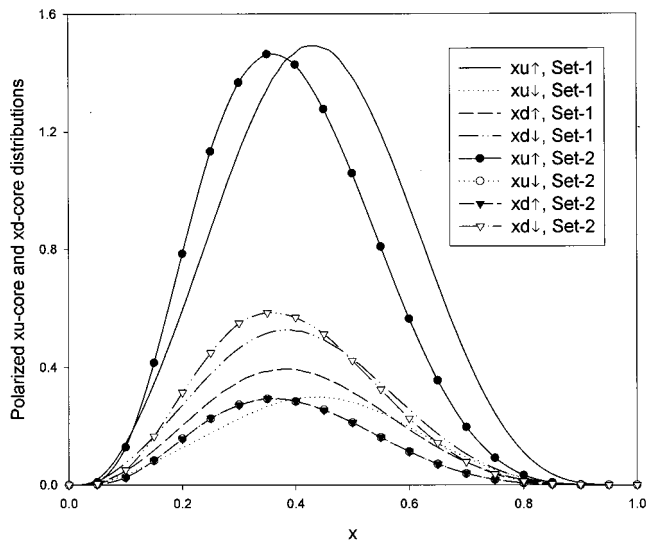


FIG. 1. Polarized xu -core and xd -core distributions for set 1 and set 2. Set 1 represents a diquark-quark distribution while in set 2 there is no quark clusterization.

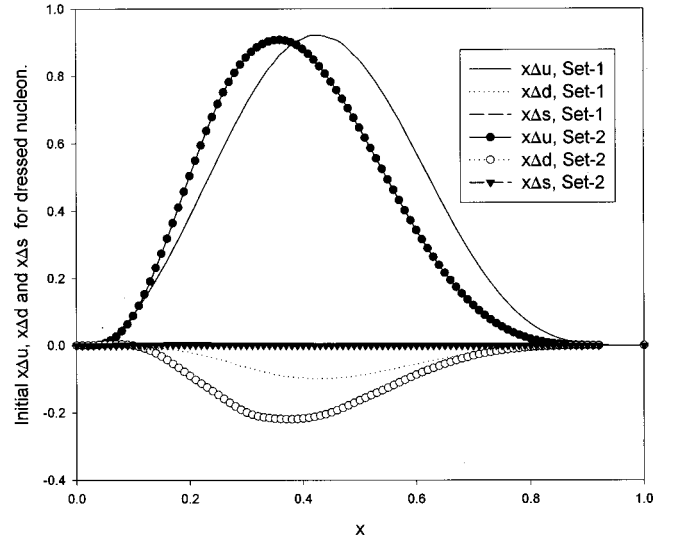


FIG. 2. Initial $x\Delta u$, $x\Delta d$, and $x\Delta s$ for dressed nucleon. Set 1 represents a diquark-quark distribution while in set 2 there is no quark clusterization.

tors [79,80] to final momentum transferred and compared with experimental results. The code uses the modified minimal subtraction ($\overline{\text{MS}}$) renormalization scheme and calculates Q^2 evolution to the next-to-leading order of the running coupling constant with QCD scale parameter of 0.2 GeV. The evolved distributions of Figs. 2–4, respectively, are shown in Figs. 5–7. We have used evolution parameter $t=0.3$ and have assumed that there is no initial gluon polarization. With the exception of the expected shift to lower x the general features are the same preevolution. For example, in Fig. 3 the polarized strange quark distributions peak at about $x=0.2$ and peak value of about 0.0022. In Fig. 6 the polarized distributions of the strange quarks after evolution peak at about $x=0.1$ and peak value of about 0.0065, but the total strange

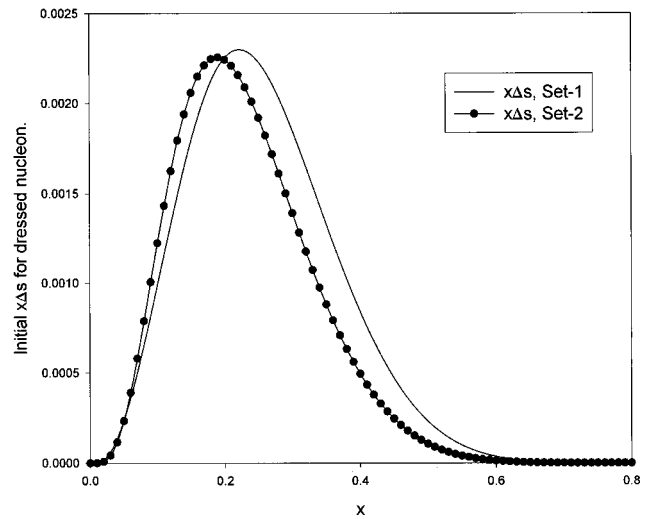


FIG. 3. Initial $x\Delta s$ for dressed nucleon. Set 1 represents a diquark-quark distribution while in set 2 there is no quark clusterization.

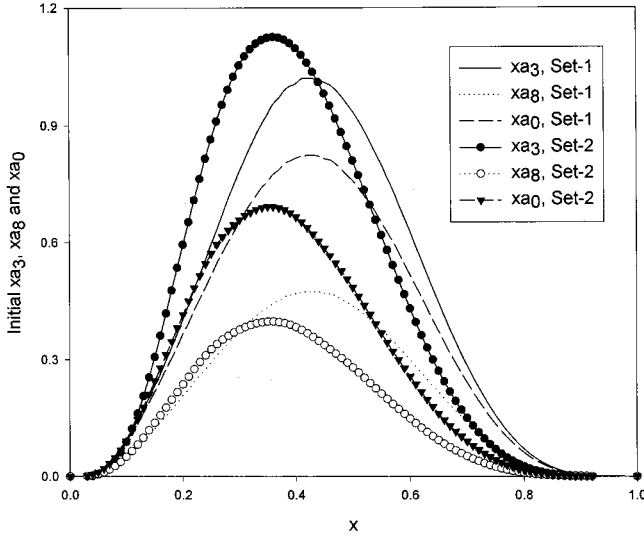


FIG. 4. Initial x_{a_3} , x_{a_8} , and x_{a_0} . Set 1 represents a diquark-quark distribution while in set 2 there is no quark clusterization.

quark polarization remains roughly the same at about 0.015. We know that evolution generates gluon polarization. In set 1 we get $\Delta G=0.66$ and in set 2 we get $\Delta G=1.21$. For the sake of consistency we renormalize total gluon polarization for both sets to be 2.5. Although this seems to be a rather high contribution, it is not unexpected in PQCD but it should be considered as absolute upper limit as explained by Ellis and Karliner [34]. As mentioned in the Introduction the experimental observation is actually a superposition of quark and gluon polarization. Taking this into account one can write

$$\Delta q \rightarrow \Delta q - \frac{\alpha_s}{2\pi} \Delta G, \quad (22)$$

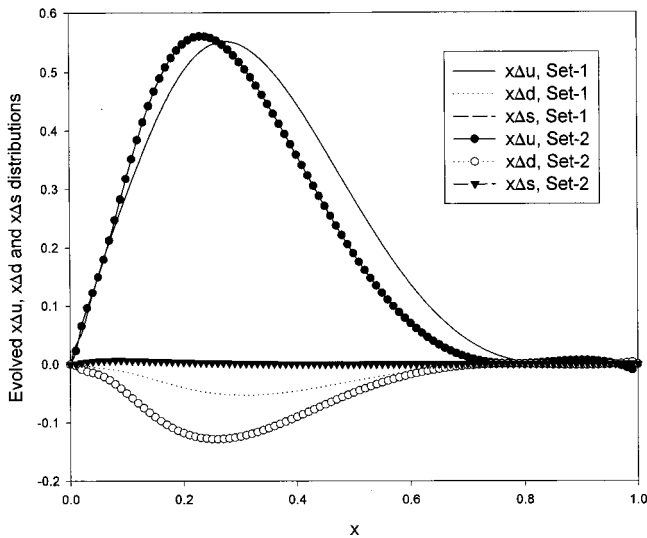


FIG. 5. Evolved $x_{\Delta u}$, $x_{\Delta d}$, and $x_{\Delta s}$ distributions with evolution parameter $t = 0.3$. Set 1 represents a diquark-quark distribution while in set 2 there is no quark clusterization with no corrections due to gluon anomaly.

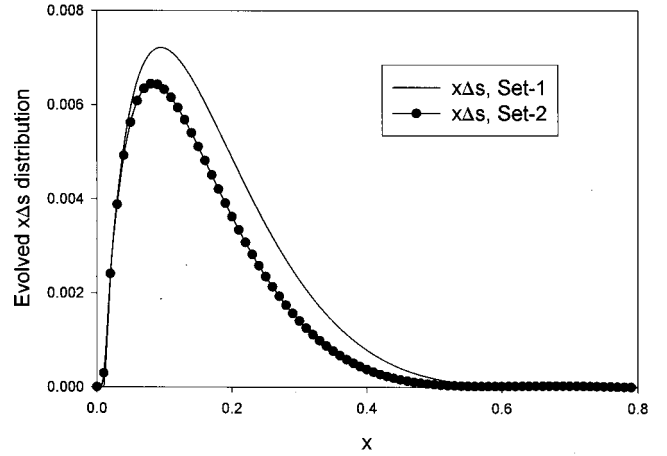


FIG. 6. Evolved $x_{\Delta s}$ with evolution parameter $t=0.3$. Set 1 represents a diquark-quark distribution while in set 2 there is no quark clusterization with no corrections due to gluon anomaly.

where α_s is QCD running coupling constant and in our case we choose $\alpha_s/2\pi=0.048$ which relates to Q^2 , about 4 GeV^2 . The results of taking into account Eq. (22) are shown in Figs. 8 and 9. As can be seen in Fig. 8 this effect clearly results in negative strange sea-quark polarization. In Figs. 8 and 9 we also present plots generated by using quark distributions parametrized by asymmetry analysis collaboration (AAC) group. AAC has generated their distributions by fitting the world experimental data and gives analytical expressions at $Q^2=1 \text{ GeV}^2$ [84]. The plots in Figs. 8 and 9 are generated by evolving the initial AAC distributions using the evolution parameter $t=0.1$. As can be seen in Fig. 8 both of our models overestimate the contribution of the u quark to the nucleon polarization. For the d quark set 2 is in reasonably good agreement with the AAC result. Figure 9 repre-

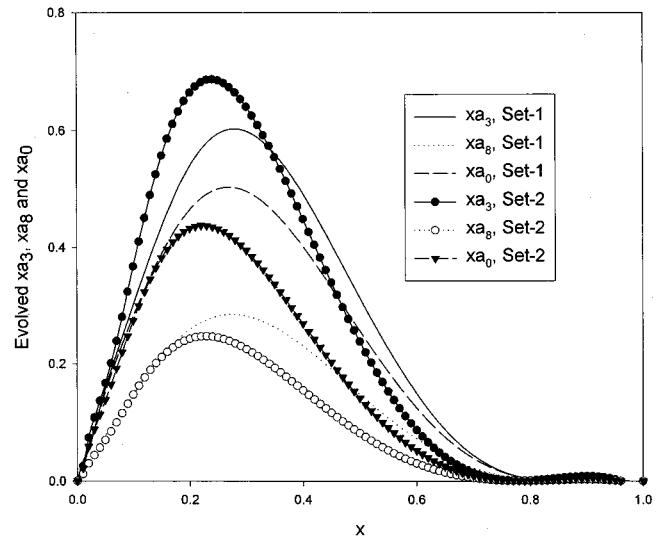


FIG. 7. Evolved x_{a_3} , x_{a_8} , and x_{a_0} with evolution parameter $t = 0.3$. Set 1 represents a diquark-quark distribution while in set 2 there is no quark clusterization with no corrections due to gluon anomaly.

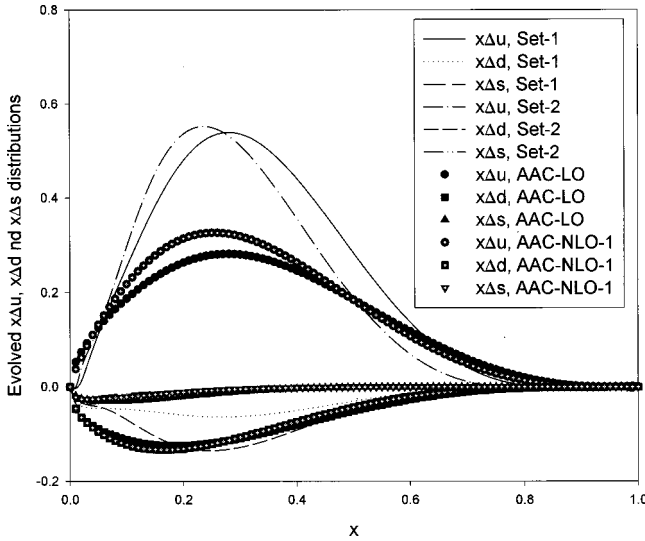


FIG. 8. Evolved $x\Delta u$, $x\Delta d$, and $x\Delta s$ distributions. Set 1 represents diquark-quark distribution while in set 2 there is no quark clusterization with corrections due to gluon anomaly. AAC-LO and AAC-NLO-1 plots have been generated using leading order and next-to-leading order calculations of quark distributions by AAC group, respectively (Ref. [84]).

sents high resolution plots for strange quark distributions. Again, for this case set 2 is in reasonable agreement with the next-to-leading order calculation of the AAC group. Our numerical results along with some experimental and theoretical results are presented in Table II. There are a few points to be made concerning this data. Set 1 even after the introduction of gluon anomaly results in rather small magnitude of Δd and positive first moment of g_1^n , which is in contrast with observation [9,17,18]. However, it reproduces strange quark

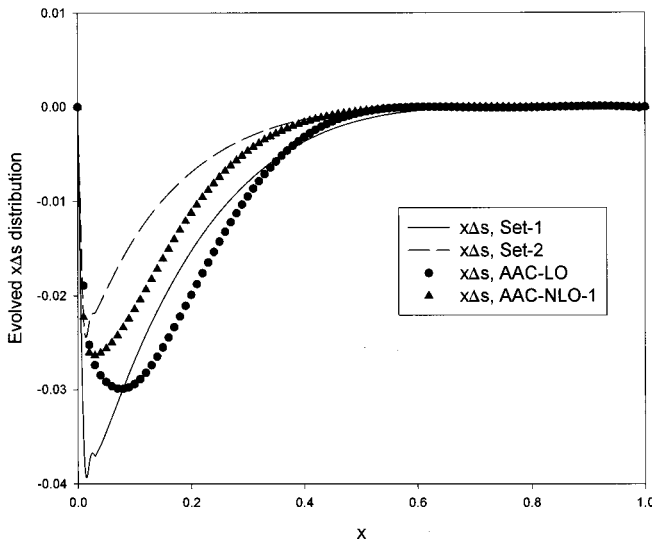


FIG. 9. Evolved $x\Delta s$ distributions. Set 1 represents a diquark-quark distribution while in set 2 there is no quark clusterization with corrections due to gluon anomaly. AAC-LO and AAC-NLO-1 plots have been generated using leading order and next-to-leading order calculations of quark distributions by AAC group, respectively (Ref. [84]).

TABLE II. Comparison of the results of our models with theory and experiment. The first three rows are experimental results corresponding to Refs. [18,17,9], respectively. The fourth row corresponds to Ellis-Jaffe [27] and Bjorken [25,26] sum rules. Row five is simply the nonrelativistic quark parton model prediction. The sixth row corresponds to relativistic quark model calculations [83]. The results of our work are presented in the last four rows.

	Δu	Δd	Δs	Γ_1^p	Γ_1^n	$\Gamma_1^p - \Gamma_1^n$
E143 (3 GeV ²)	0.83	-0.43	-0.09	0.133	-0.032	0.165
E154 (5 GeV ²)				0.122	-0.056	0.168
SMC (5 GeV ²)				0.132	-0.048	0.181
EJSR/BSR				0.167	-0.015	0.182
NRQPM ($\Delta G=0$)	1.33	-0.33	0			
RQPM ($\Delta G=0$)	1.0	-0.25	0			
Set 1 ($\Delta G=0$)	1.04	-0.075	0.015	0.228	0.042	0.186
Set 2 ($\Delta G=0$)	1.02	-0.199	0.014	0.216	0.013	0.203
Set 1 ($\Delta G \neq 0$)	0.917	-0.195	-0.105	0.187	0.002	0.185
Set 2 ($\Delta G \neq 0$)	0.951	-0.271	-0.059	0.193	-0.011	0.204

polarization and BSR rather nicely. Set 2 reproduces a more reasonable Δd and first moment of g_1^n but somewhat overestimates BSR. The important point is that when one compares the last two rows of Table II with other theoretical calculations (NRQPM and RQPM rows) one realizes that introduction of meson cloud in relativistic quark model results in better agreement with experiment which once again shows the significance of the role of meson cloud in nucleon structure.

One final comment is that in Ref. [76] we calculated the F_2 structure function for the nucleon using the same approach as we have done in the present work. There we showed that a diquark-quark distribution which is dominated by a spin-0 diquark makes it possible to have reasonable agreement with experiment. In contrast with a core nucleon where there is no clusterization of quarks, and calculated F_2 structure function consistently undershoots observation rather significantly in the medium to high x range. However, in this case although the results are mixed for both sets, it seems that set 2 is in better agreement with experiment. Therefore, for a diquark-quark model to consistently describe polarized and unpolarized cases, one may have to include the effects of a spin-1 diquark. What is common between the previous work and the present one is, once again, the important role of meson cloud in nucleon.

APPENDIX

The explicit form of the vertex function $V_{\text{IMF}}^{\lambda\lambda'}(y, k_\perp^2)$ used in Eq. (14b) is

$$V_{\text{IMF}}^{\lambda\lambda'}(y, k_\perp^2) = |\Gamma_{MB}(M_{MB}^2)|^2 V'_{\text{IMF}}{}^{\lambda\lambda'}(y, k_\perp^2), \quad (\text{A1})$$

where $\Gamma_{MB}(M_{MB}^2)$ is the vertex form factor and is parametrized by the exponential function of the invariant mass M_{MB} of the intermediate baryon-meson state

$$\Gamma_{MB}(M_{MB}^2) = e^{-(M_{MB}^2 - m_N^2)/\Lambda_{MB}^2}, \quad (\text{A2})$$

where λ_{MB} are free parameters which are determined by fitting experimental data. In the following we present the explicit form of $V'_{\text{IMF}}{}^{\lambda\lambda'}(y, k_{\perp}^2)$, for intermediate helicity states of pseudoscalar meson and baryon states. The complete list can be found in the original work presented in Refs. [69,72]. For intermediate states $N\pi$, $N\eta$, ΣK , and ΛK the vertex functions are

$$\frac{1}{2} \rightarrow +\frac{1}{2}, \quad 0 \quad \frac{g_{NMB}}{2} \frac{ym_N - m_B}{\sqrt{ym_N m_B}}, \quad (\text{A3})$$

$$\frac{1}{2} \rightarrow -\frac{1}{2}, \quad 0 \quad \frac{g_{NMB} e^{-i\phi}}{2} \frac{k_{\perp}}{\sqrt{ym_N m_B}}, \quad (\text{A4})$$

and the following represent those for $\Delta\pi, \Sigma^*K$ intermediate states:

$$\frac{1}{2} \rightarrow +\frac{3}{2}, \quad 0 \quad -\frac{g_{NMB} e^{+i\phi}}{2\sqrt{2}} \frac{k_{\perp}(ym_N + m_B)}{y\sqrt{ym_N m_B}}, \quad (\text{A5})$$

$$\frac{1}{2} \rightarrow +\frac{1}{2}, \quad 0 \quad \frac{g_{NMB}}{2\sqrt{6}} \frac{(ym_N + m_B)^2(ym_N - m_B) + k_{\perp}^2(ym_N + 2m_B)}{ym_B \sqrt{ym_N m_B}}, \quad (\text{A6})$$

$$\frac{1}{2} \rightarrow -\frac{1}{2}, \quad 0 \quad \frac{g_{NMB} e^{-i\phi}}{2\sqrt{6}} \frac{k_{\perp} [(ym_N + m_B)^2 - 3m_B(ym_N + 2m_B) + k_{\perp}^2]}{ym_B \sqrt{ym_N m_B}}, \quad (\text{A7})$$

$$\frac{1}{2} \rightarrow -\frac{3}{2}, \quad 0 \quad -\frac{g_{NMB} e^{-2i\phi}}{2\sqrt{2}} \frac{k_{\perp}^2}{y\sqrt{ym_N m_B}}. \quad (\text{A8})$$

In the above equations we have used the notation $1/2 \rightarrow \lambda, \lambda'$, where λ and λ' are the helicities of the baryon and meson, respectively. y is the longitudinal momentum fraction of the baryon and ϕ is the angle between the baryon's transverse momentum and that of the nucleon. g_{MB} are the coupling constants which we choose [57,69] $g_{p\pi^0 p}^2 = 13.6$ and $g_{p\Delta^+ + \pi^-}^2 = 10.85 \text{ GeV}^{-2}$. Other coupling constants are related to these two through the quark model [69,81,82].

-
- [1] J. Ashman *et al.*, Phys. Lett. B **206**, 364 (1988).
[2] J. Ashman *et al.*, Phys. Lett. B **328**, 1 (1989).
[3] B. Adeva *et al.*, Phys. Lett. B **302**, 533 (1993).
[4] D. Adams *et al.*, Phys. Lett. B **329**, 399 (1994).
[5] D. Adams *et al.*, Phys. Lett. B **357**, 533 (1995).
[6] D. Adams *et al.*, Phys. Lett. B **396**, 338 (1997).
[7] D. Adams *et al.*, Phys. Rev. D **56**, 5330 (1997).
[8] B. Adeva *et al.*, Phys. Lett. B **412**, 414 (1997).
[9] B. Adeva *et al.*, Phys. Rev. D **58**, 112001 (1998).
[10] B. Adeva *et al.*, Phys. Rev. D **60**, 072004 (1999).
[11] J. Le Goff *et al.*, Phys. Lett. A **666**, 296 (2000).
[12] P. L. Anthony *et al.*, Phys. Rev. Lett. **71**, 959 (1993).
[13] P. L. Anthony *et al.*, Phys. Rev. D **54**, 6620 (1996).
[14] K. Abe *et al.*, Phys. Rev. Lett. **74**, 346 (1995).
[15] K. Abe *et al.*, Phys. Rev. Lett. **75**, 25 (1995).
[16] K. Abe *et al.*, Phys. Lett. B **364**, 61 (1995).
[17] K. Abe *et al.*, Phys. Rev. Lett. **79**, 26 (1997).
[18] K. Abe *et al.*, Phys. Rev. D **58**, 112003 (1998).
[19] P. L. Anthony *et al.*, Phys. Lett. B **463**, 339 (1999).
[20] O. Rondon, Nucl. Phys. A **663**, 293 (1997).
[21] K. Ackerstaff *et al.*, Phys. Lett. B **404**, 383 (1997).
[22] A. Airapetian *et al.*, Phys. Lett. B **442**, 484 (1998).
[23] A. Simon *et al.*, Nucl. Phys. B (Proc. Suppl.) **86**, 112 (2000).
[24] A. Brull *et al.*, Nucl. Phys. A **663**, 2000 (2000).
[25] J. D. Bjorken, Phys. Rev. **148**, 1467 (1966).
[26] J. D. Bjorken, Phys. Rev. D **1**, 1376 (1970).
[27] J. Ellis and R. Jaffe, Phys. Rev. D **9**, 1444 (1974).
[28] G. Altarelli and G. G. Ross, Phys. Lett. B **212**, 391 (1988).
[29] R. D. Carlitz, J. C. Collins, and A. H. Mueller, Phys. Lett. B **214**, 299 (1988).
[30] A. V. Efremov, J. Soffer, and O. V. Teryaev, Nucl. Phys. B **246**, 97 (1990).
[31] G. T. Bodwin and J. Qiu, Phys. Rev. D **41**, 2755 (1990).
[32] S. D. Bass and A. W. Thomas, J. Phys. G **19**, 639 (1993).
[33] H. Y. Cheng, Chin. J. Phys. (Taipei) **38**, 753 (2000).
[34] J. Ellis and M. Karliner, hep-ph/9601280.
[35] R. L. Jaffe and A. Manohar, Nucl. Phys. B **337**, 509 (1990).
[36] M. Anselmino, A. Efremov, and E. Leader, Phys. Rep. **261**, 1 (1995).
[37] V. U. Stiegler, Phys. Rep. **277**, 1 (1996).
[38] I. Hinchliffe and A. Kwiatkowski, Annu. Rev. Nucl. Part. Sci. **46**, 609 (1996).
[39] G. P. Ramsey, Prog. Part. Nucl. Phys. **39**, 599 (1997).
[40] L. F. Li and T. P. Cheng, hep-ph/9709293.
[41] G. Altarelli, R. D. Ball, S. Forte, and G. Ridolfi, Acta Phys. Pol. B **29**, 1145 (1998).
[42] M. C. Vetterli, hep-ph/9812420.
[43] J. Kodaira and K. Tanaka, Prog. Theor. Phys. **101**, 191 (1999).

- [44] B. Lampe and E. Reya, Phys. Rep. **332**, 1 (2000).
[45] P. A. M. Dirac, Rev. Mod. Phys. **21**, 392 (1949).
[46] H. Leutwyler and J. Stern, Ann. Phys. (N.Y.) **112**, 94 (1978).
[47] M. G. Fuda, Ann. Phys. (N.Y.) **197**, 265 (1990).
[48] M.G. Fuda, Ann. Phys. (N.Y.) **231**, 1 (1994).
[49] M. Burkardt, Ann. Math. **23**, 1 (1996).
[50] F. Schlumpf, Ph.D. thesis, University of Zurich, 1992.
[51] F. Schlumpf, Phys. Rev. D **47**, 4114 (1993).
[52] V. B. Berestetskii and M. V. Terent'ev, Sov. J. Nucl. Phys. **24**, 547 (1976).
[53] V. B. Berestetskii and M. V. Terent'ev, Sov. J. Nucl. Phys. **25**, 347 (1977).
[54] F. E. Close, Phys. Lett. **43B**, 422 (1973).
[55] A. De Rujula, H. Georgi, and S. L. Glashow, Phys. Rev. D **12**, 147 (1970).
[56] H. J. Melosh, Phys. Rev. D **9**, 1095 (1974).
[57] V. R. Zoller, Z. Phys. C **53**, 443 (1992).
[58] A. W. Schreiber, P. J. Mulders, A. I. Signal, and A. W. Thomas, Phys. Rev. D **45**, 3069 (1992).
[59] W. Y. P. Hwang and J. Speth, Phys. Rev. D **46**, 1198 (1992).
[60] A. W. Thomas and W. Melnitchouk, *New Frontiers in Nuclear Physics* (World Scientific, Singapore, 1993), p. 41.
[61] A. Szczurek and J. Speth, Nucl. Phys. **A555**, 249 (1993).
[62] A. Szczurek, J. Speth, and G. T. Garvey, Nucl. Phys. **A570**, 765 (1994).
[63] N. N. Nikolaev, A. Szczurek, J. Speth, and V. R. Zoller, Z. Phys. A **349**, 59 (1994).
[64] B. C. Pearce, J. Speth, and A. Szczurek, Phys. Rep. **242**, 193 (1994).
[65] F. M. Steffens, H. Holtmann, and A. W. Thomas, Phys. Lett. B **358**, 139 (1995).
[66] W. Melnitchouk and A. W. Thomas, Z. Phys. A **353**, 311 (1995).
[67] A. Szczurek, M. Ericson, H. Holtmann, and J. Speth, Nucl. Phys. **A596**, 397 (1996).
[68] A. Szczurek, A. J. Buchmann, and A. Faessler, J. Phys. G **22**, 1741 (1996).
[69] H. Holtmann, A. Szczurek, and J. Speth, Nucl. Phys. **A596**, 631 (1996).
[70] S. J. Brodsky and Bo-Qiang Ma, Phys. Lett. B **381**, 371 (1996).
[71] W. Koepf, L. L. Frankfurt, and M. Strikman, Phys. Rev. D **53**, 2586 (1996).
[72] J. Speth and A. W. Thomas, Adv. Nucl. Phys. **24**, 83 (1997).
[73] F. M. Steffens and A. W. Thomas, Phys. Rev. C **55**, 900 (1997).
[74] S. D. Bass and D. Schutte, Z. Phys. A **357**, 85 (1997).
[75] S. Kumano, Phys. Rep. **303**, 183 (1998).
[76] F. Zamani, Phys. Rev. C **58**, 3641 (1998).
[77] Z. Dziembowski, C. J. Martoff, and P. Zyla, Phys. Rev. D **50**, 5613 (1994).
[78] G. Altarelli and G. Parisi, Nucl. Phys. **B126**, 298 (1977).
[79] S. Kumano and J. T. Londergan, Comput. Phys. Commun. **69**, 373 (1992).
[80] R. Kobayashi, M. Konuma, and S. Kumano, Comput. Phys. Commun. **86**, 264 (1995).
[81] B. Holzenkamp, K. Holinde, and J. Speth, Nucl. Phys. **A500**, 485 (1989).
[82] G.E. Brown and W. Weise, Phys. Rep., Phys. Lett. **22**, 281 (1975).
[83] S. J. Brodsky and F. Schlumpf, Phys. Lett. B **329**, 111 (1994).
[84] Y. Goto *et al.*, Phys. Rev. D **62**, 034017 (2000).